Astron. Astrophys. 327, L9–L12 (1997)

ASTRONOMY AND ASTROPHYSICS

LETTER

Letter to the Editor

Chemical stratification in the Orion Bar region: CN and CS submillimeter observations

R. Simon[1], **J. Stutzki**[1], **A. Sternberg**[2], **and G. Winnewisser**[1]

[1] I. Physikalisches Institut, Universität zu Köln, Zülpicher Straße 77, D-50937 Köln, Germany
[2] School of Physics and Astronomy, Tel Aviv University, Ramat Aviv 69978, Israel

Received 21 July 1997 / Accepted 7 August 1997

Abstract. We present fully sampled spectral line maps of the Orion Bar region observed simultaneously in the CN N=3→2 and CS J=7→6 rotational transitions with the JCMT at an angular resolution of 14″. We find that the CN emission specifically traces an intermediate cloud layer located between the peaks of vibrationally excited H_2 and HCO^+ emission located closer to the ionization front, and CS emission originating closer to the cloud core. By comparing the observed spatial displacement of CN and CS emission with PDR models we infer a density of $\sim 2\times10^5 cm^{-3}$ for these cloud layers. This value is in agreement with the results of an escape probability radiative transfer analysis of our CN and CS line observations. We conclude that the observed distribution of H_2/CN/CS is consistent with chemical stratification in an edge-on PDR in which high density gas ($\sim 2\times10^5 cm^{-3}$) is distributed homogeneously.

Key words: ISM: abundances – ISM: clouds – ISM: individual objects: Orion Bar – ISM: molecules – ISM: structure – Radio lines: ISM

1. Introduction

Photon-dominated regions (PDRs) are found in a variety of Galactic and extragalactic sources with significant variation in the incident far ultraviolet (FUV) flux and the gas density. They show bright emission in their most important UV excited and cooling lines (in sequence according to the distance from the edge of the molecular cloud), namely fluorescent vibrational molecular hydrogen (H_2^*) lines, the atomic fine structure transitions of [CII] at 158μm and [OI] at 63μm, and in mm/submm emission lines of [CI], CO and other molecular species.

The Orion Bar region is widely considered as a prototype of an edge-on PDR associated with a dense molecular cloud. It is exposed to a high flux of FUV photons from the Trapezium cluster, a group of young OB stars, which is located at a projected distance of 0.25 pc from the ionization front (IF), outlined by radio continuum emission (Yusef-Zadeh 1990) ($\chi\sim 4\times10^4$ in units of the standard interstellar radiation field (Draine 1978) at the edge of the IF (see e.g. Tielens & Hollenbach 1985b and van der Werf et al. 1996 (vdW96)).

Recent model calculations (Sternberg & Dalgarno 1995 (SD95), Jansen et al. 1995) predict that homogeneous (i.e. constant density) PDRs consist of several distinct chemical zones each governed by specific sets of chemical reactions and decreasing photodissociation and photoionization rates. For example, in the model presented by SD95, HCO^+ and CN molecules are abundant in zones closer to the PDR surface where the UV radiation field is only partly attenuated, whereas CS and HCN become abundant at larger (and more shielded) cloud depths closer to the cloud core.

Due to its proximity (∼460 pc), the Orion Bar is a unique region to study the morphology and chemical composition of a dense PDR and to resolve a possible stratified emission distribution. Consequently, many interstellar species and transitions have been observed at a great variety of frequencies towards this source (see e.g. Tauber et al. 1994, 1995, Störzer et al. 1995, vdW96, Hogerheijde et al. 1995, White & Sandell 1995, and references therein). Many efforts have been made to derive a consistent interpretation of the observations using theoretical models which consider either homogeneous gas distributions or a combined clump-interclump morphology (e.g. Tielens & Hollenbach 1985a, Köster et al. 1994, Sternberg & Dalgarno 1989, 1995, Hogerheijde et al. 1995, Tauber et al. 1994, 1995, vdW96). In the latter case, the attenuation of the FUV radiation is provided by the interclump material (with a density of typically 5×10^4 cm^{-3}) and emission from high density tracers arises from small embedded high density ($> 10^6$ cm^{-3}) clumps. Hogerheijde et al. (1995) attribute the observed molecular column density enhancement towards the Bar to a change from face-on to edge-on and back to face-on geometry.

Send offprint requests to: R. Simon

The CN radical with its dipole moment of 1.45 Debye (comparable to 1.96 Debye for CS) serves as a probe for high density molecular material. Assuming CS collisional rate coefficients (Green & Chapman 1978) to be appropriate for CN, the critical density of the N=3→2 transition is $\sim 9\times10^6$ cm^{-3} ($\sim 3\times10^7$ cm^{-3} for CS J=7→6). The rotational transitions of CN exhibit simultaneously observable fine and hyperfine structure (hfs) which allows direct determination of the optical depth from the relative line intensities. Column densities in the energy levels connected to the observed transitions are thus determined without assuming isotopic abundances and without possible ambiguities due to high optical depth.

In this *Letter* we present maps of the CN and CS integrated intensities and discuss their spatial distribution perpendicular to the IF. We use the observed spatial displacement of the CN and CS emission maxima together with PDR models and assume an edge-on geometry to infer the density of the emitting gas. Molecular abundances from the model in conjunction with results of a (single-component) escape-probability analysis are used to derive the line-of-sight thickness of the edge-on PDR.

2. Observations

The CN and CS submillimeter observations were obtained at the James Clerk Maxwell Telescope (JCMT)[1] on Mauna Kea, Hawaii, during one shift in February 1995. The hfs pattern of CN N=3→2 (340247.90 MHz for the strongest hfs component) was observed simultaneously with the CS J=7→6 transition (342882.95 MHz) from the other sideband, using the B3i SIS receiver. This procedure guarantees identical pointing between the two line maps. Fig. 1 shows a spectrum recorded in the region of peak CN intensity. Typical system noise temperatures were 720 K, including an average atmospheric zenith opacity of 0.1. The angular resolution of the telescope at 340 GHz is 14″. Spectra at the individual map positions were obtained in an 'on the fly' fast mapping technique, scanning the source in Right Ascension at constant Declination. The resulting grid spacing was 6″ and the integration time on each source position 10s, resulting in an r.m.s. noise temperature of 0.9 K in a 0.28 km s^{-1} velocity bin. Pointing was checked regularly and found to be better than 2″. The spectra were calibrated for atmospheric attenuation with a standard chopper wheel method. We used the 500 MHz wide standard configuration of the autocorrelator, providing a channel spacing of 313 kHz. A sideband ratio of unity was assumed. The line intensities are given on a T_{mb} scale (using a value of η_{mb} = 0.68 at 340 GHz, as determined from observations of Jupiter and Mars).

3. Chemical Stratification

Fig. 2 shows the observed CN and CS intensity distribution towards the Orion Bar integrated over the relevant velocity range

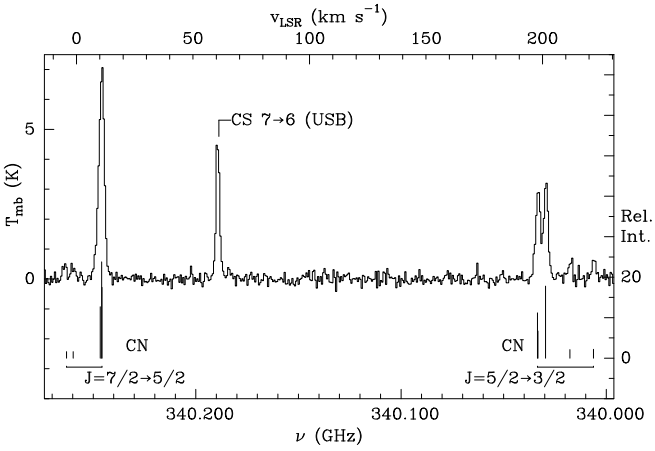

Fig. 1. CN N=3→2with the fine and hyperfine structure resolved, and CS J=7→6 in the region of peak CN intensity. The vertical bars denote the positions and low opacity intensities of the CN hfs lines.

9.5 to 12.5 km s^{-1}and a comparison of CN N=3→2 to H_2^* 2.12μm S(1) v=1→0 (vdW96) emission. The H_2^* emitting region, which marks the transition zone from atomic to molecular hydrogen, lies closest to the exciting stars, the Trapezium, located in the north-west. CS emission is produced in two prominent clumps at the north-east and south-west boundaries of the Bar (vdW96), and in a dense ridge between the clumps. However, the CN emission originates closer to the IF, and is more prominent near the UV illuminated edges of the clumps and ridge seen in CS emission. The observations thus reveal a stratified distribution of molecular emission along the direction towards the star cluster. The CN emission in the ridge is much more pronounced than in the adjacent clumps, probably indicating the significant influence of FUV radiation at this location as opposed to the clumps at the boundaries of the Bar. Fig. 3a displays the intensity profile perpendicular to the IF, derived by averaging data from the boxed region shown in Fig. 2. From this cut we infer the intensity peaks of CN and CS to be located at distances of 0.045 and 0.067 pc (20″ and 30″) respectively from the IF, whereas enhanced emission from H_2^*, HCO^+ and CO^+, as derived from similar cuts in vdW96 and Störzer et al. (1995), occurs at 0.033 pc ($\sim$15″). The distribution of the optical depth of the CN N=3→2 transition along the cut, as derived from the hfs line intensities, is shown as a third curve in Fig. 3a. It closely follows the CN intensity distribution and shows that the CN intensity maximum coincides with the location of peak CN column density.

The observed CN and CS transitions have similar critical densities but, due to the higher energy above ground level of the CS J=7 rotational level (66 K compared to 33 K for the N=3 level of CN), CS J=7→6 should trace a warmer part of the cloud, i.e. *closer* to the IF than CN N=3→2, contrary to what is observed. This suggests that the positionally displaced CN and CS emission peaks reflect actual abundance variations of chemical origin. Indeed, in the SD95 model the CN abundance is largest near the inner edge of the CII zone at a cloud depth corresponding to a visual extinction A_v=2 (where the CS abun-

[1] The JCMT is operated by The Observatories on behalf of the Particle Physics and Astronomy Research Council of the United Kingdom, the Netherlands Organisation for Scientific Research, and the National Research Council of Canada

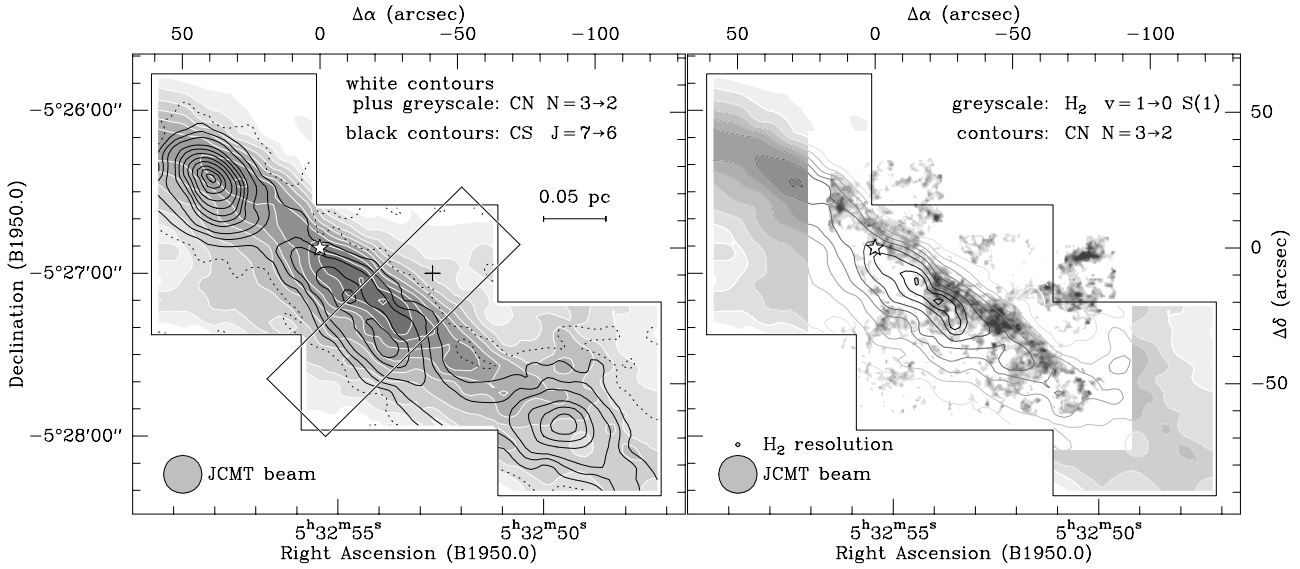

Fig. 2. CN N=3→2, CS J=7→6 (mapped area outlined by a polygon) and H_2^* v=1→0 S(1) (vdW96) emission towards the Orion Bar. Offsets are relative to θ^2A Ori ($\alpha = 5^h32^m55^s.4$, $\delta = -5°26'50''.7$). CN and CS intensities are integrated over 9.5 to 12.5 km s^{-1}, relevant for emission from the Orion Bar. Contours range from 2.4 K km s^{-1} (3σ, dashed) to 24.3 K km s^{-1} and 28.1 K km s^{-1} for CN and CS respectively in steps of 3σ. Greyscales in the H_2^* image range from 0.25 to 3.5×10^{-4} erg s^{-1} cm^{-2} sr^{-1}. The boxed area indicates the region where spectra have been averaged to create the cut presented in Fig. 3 with the cross at the position of the IF.

dance is very small) and the CS abundance is largest at the inner edge of the SI zone at A_v=8.

For the model calculations presented below, we employed the SD95 model. We adopted gas-phase oxygen and carbon abundances of 6×10^{-4} and 3×10^{-4} respectively, and a sulfur abundance of 2×10^{-7} appropriate for the Orion Bar region (Jansen et al. 1995). We used the UMIST chemical rate-coefficients listed by Millar et al. (1997) and the photo rates listed by SD95. We then calculated PDR models for a range in hydrogen density and the intensity of the FUV radiation field. The results show that for a fixed χ the separation between the CN and CS peaks remains fixed and close to ΔA_v=6 for hydrogen gas densities between 10^4 and 10^7 cm^{-3}. Similar behavior is apparent in the chemical model results for the Orion Bar presented by Jansen et al. (1995). Varying the FUV intensity (at fixed density) shifts the locations of the CN and CS density peaks relative to the cloud surface, but the separation between them again remains close to ΔA_v=6. In the following, we adopt a value of $\chi = 4\times10^4$ at the edge of the IF. Using the canonical value of $\langle N(H) + 2N(H_2)\rangle = 1.9\times10^{21}$ cm^{-2} per magnitude of visual extinction (Bohlin et al., 1978) and a distance of 460 pc, the calculated shift between the peaks is translated to a linear scale in the cloud and, together with the observed displacement, constrains the density of a homogeneous edge-on PDR to 1–4×10^5cm^{-3}.

The absolute chemical abundances resulting from the models have to be treated with caution since the use of different chemical and photo rates may, for certain species like CN, result in differences as large as an order of magnitude. However, the quantities from the modified SD95 model presented here agree with the values reported by Jansen et al. (1995) to within a factor

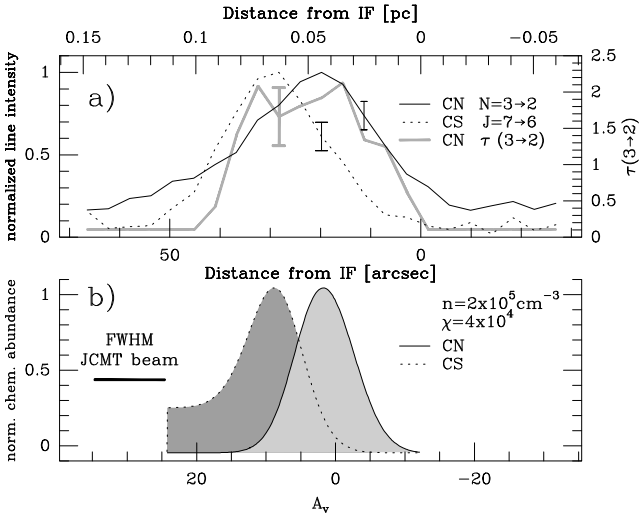

Fig. 3. a CN N=3→2 and CS J=7→6 emission profile and CN N=3→2 optical depth (right axis) along the cut marked in Fig. 2. Typical 1σ error bars are indicated. **b** Normalized abundances from the modified SD95 model with the given parameters and convolved with the JCMT 14″ beam.

of 4 for CN and 2 for CS. The model abundances of CN and CS (normalized to their peak values) calculated for χ=4×10^4 and n_{H_2}=2×10^5cm^{-3} and convolved with the 14″ JCMT beam are shown in Fig. 3b. The extent of the lower excitation CN emission beyond the boundaries of the Bar, as seen in the cut, might be attributed to emission from the back surface of the cavity walls seen face-on, and supports the global geometrical

picture of the PDR changing from face-on to edge-on and back to face-on, as proposed by Hogerheijde et al. (1995).

The arguments up to here are based on the relative displacement between the CN and CS emission peaks only. Shifting the chemical model results in position to coincide with the observed peaks, we see that, provided the absolute pointing in our observations is accurate, the location of the IF does not coincide with the zero point of the A_v scale in the chemical model (Fig. 3). This suggests that the FUV attenuation within the first $\sim 2A_v$ of the cloud may be provided by lower density material, where an average PDR model density of $\sim 3\times10^4$cm^{-3} is appropriate to account for the offset between the distance and the A_v scale. vdW96 analyzed CS line ratios and confirmed with a completely different method that there is a density enhancement at the CS layer. The densities agree very well with the values we derived. A lower density regime is expected at the interface, since the density should increase gradually from the cavity around the Trapezium, devoid of molecules, to the molecular cloud. Emission of specific high density tracers in this region is interpreted to originate from high density clumps with low volume filling factors embedded in the lower density material providing the UV attenuation. Such a picture is readily supported by the high degree of fragmentation in the H_2^* image between the IF and the CN emission peak.

4. Excitation Analysis

We used a single component escape probability code (Stutzki & Winnewisser 1985) together with our CN N=3→2 and CS J=7→6 data, the CN N=1→0, N=2→1 and CS J=5→4 observations reported by Fuente et al. (1996) and vdW96, as well as the CN optical depths from the hyperfine fits, to determine the hydrogen gas density and CN and CS column density in the emitting region. For the unknown CN collisional rate coefficients we adopted the CS rates from Green & Chapman (1978). We considered kinetic temperatures of 40–100 K to be appropriate for the Bar material. From the intensity ratios of the rotational transitions and the CN optical depths, we infer hydrogen densities of 1–4$\times10^5$cm^{-3} for the CN and the CS peak. Moreover, the absolute line intensities of CN N=3→2 and CS J=7→6 imply beam filling factors of unity. Values for the CN and CS column density 20″ (and 30″) from the IF are determined to be 1×10^{14} (2×10^{14}) and 5×10^{13} (5×10^{14}) cm^{-2} respectively.

The absolute values of the molecular abundances from the SD95 model, convolved with the JCMT beam, take values of 6×10^{-10} and 1×10^{-9} for CN and CS respectively at the CN maximum and 2×10^{-10} and 4×10^{-10} at the CS peak. Together with the molecular column densities from the escape probability analysis, this results in molecular hydrogen column densities of $1-2\times10^{23}$ cm^{-2}. At a homogeneous density of 2×10^5 cm^{-3}, the line of sight thickness of the edge-on PDR is determined to 0.16–0.27 pc (or 70″–120″), which compares well with independent results obtained by Werner et al. (1976, 0.12 pc) and Jansen et al. (1995, 0.6 pc). Assuming a width of the PDR of 0.07 pc (or 30″which corresponds to the width at half maximum in the cut), this results in an aspect ratio of 2–4.

5. Conclusions

The observed stratified distribution and the enhancement of certain chemical species towards the edge of the Orion Bar can adequately be modelled within the framework of an edge-on PDR with a homogeneous density distribution at 1–4$\times10^5$cm^{-3}. Results from an escape probability radiative transfer analysis of various CN and CS lines suggest densities in the same range and beam filling factors of unity, further supporting the homogeneous nature of the edge-on part of the Orion Bar PDR in the derived density regime.

Our observations and modelling give clear evidence for homogeneous high density gas at the edge-on part of the Orion Bar PDR. These results do not exclude the presence of embedded higher density clumps, as suggested by observations of specific high density tracers or CO^+ (Störzer et al. 1995), but, due to their low volume filling factor, these clumps do not affect the chemistry and the thickness of the PDR.

The derived density is thus substantially higher than that proposed by Hogerheijde et al. (1995), who infer values of 1–4$\times10^4$cm^{-3} for the homogeneous gas. Additional extended emission beyond the boundaries of the Bar agrees with their global scenario of a PDR changing from face-on to edge-on and back to face-on.

Acknowledgements. The authors thank the JCMT staff for their kind assistance during the observing period and Paul P. van der Werf for providing the H_2^* image. A. Fuente contributed the CN N=1→0 and N=2→1 spectra used in our radiative transfer calculations. This work was supported in part by the Deutsche Forschungsgemeinschaft via grant SFB-301. A.S. thanks the Israel Science Foundation for support.

References

Bohlin, R.C., Savage, B.D., Drake, J.F., 1978, ApJ, 224, 132
Draine, B.T., 1978, ApJS, 36, 595
Fuente, A., Rodríguez-Franco, A., Martín-Pintado, J., 1996, A&A, 312, 599
Green, S., Chapman, S., 1978, ApJS, 37, 169
Hogerheijde, M.R., Jansen, D.J., van Dishoeck, E.F., 1995, A&A, 294, 792
Jansen, D.J., Spaans. M., Hogerheijde, M.R., van Dishoeck, E.F., 1995, A&A, 303, 541
Köster, B., Störzer, H., Stutzki, J., Sternberg, A., 1994, A&A, 284, 545
Millar, T.J., Farquhar, P.R.A., Willacy, K., 1997, AAS, 121, 139
Sternberg, A., Dalgarno, A., 1989, ApJ, 338, 197
Sternberg, A., Dalgarno, A., 1995, ApJS, 99, 565, SD95
Störzer, H., Stutzki, J., Sternberg, A., 1995, A&A, 296, L9
Stutzki, J., Winnewisser, G., 1985, A&A, 144, 13
Tauber, J.A., Tielens, A.G.G.M., Meixner, M., Goldsmith, P.F., 1994, ApJ, 422, 136
Tauber, J.A., Lis, D.C., Keene, J., Schilke, P., Büttgenbach, T.H., 1995, A&A, 297, 567
Tielens, A.G.G.M., Hollenbach, D., 1985a, ApJ, 291, 722
Tielens, A.G.G.M., Hollenbach, D., 1985b, ApJ, 291, 747
van der Werf, P.P., Stutzki, J., Sternberg, A., Krabbe, A., 1996, A&A, 313, 633, vdW96
Werner, M.W., Gatley, I., Harper, D.A., Becklin, E.E., Loewenstein, R.F., Telesco, C.M., Thronson, H.A., 1976, ApJ, 204, 420
White, G.J., Sandell, G., 1995, A&A, 299, 179
Yusef-Zadeh, F., 1990, ApJ, 361, L19